Manuscript under review for journal Atmos. Meas. Tech.

Discussion started: 30 November 2018 © Author(s) 2018. CC BY 4.0 License.





1 Reactive mercury flux measurements using cation exchange membranes

- 2 Matthieu B. Miller^{1*}, Mae S. Gustin², Grant C. Edwards^{1,3}
- 3 ¹Faculty of Science and Engineering, Department of Environmental Science, Macquarie University, Sydney, NSW,
- 4 2113, Australia
- Department of Natural Resources and Environmental Science, University of Nevada, Reno NV, 89557, United
- 6 State
- 7 ³Deceased 10 September 2018.
- 8 Correspondence to: Mae Sexauer Gustin mgustin@cabnr.unr.edu

9 ABSTRACT

- A method was developed to measure gaseous oxidized mercury (GOM) air-surface exchange
 using 2 replicated dynamic flux chambers (DFCs) in conjunction with cation exchange
 membrane (CEM) filters. The experimental design and method was developed and tested in a
 laboratory setting, using materials collected from industrial scale open pit gold mines in central
 Nevada, USA. Materials used included waste rock, heap leach ore, and tailings, with substrate
- 15 concentrations ranging from 0.1 to 40 μg g⁻¹ total mercury (THg). CEM filters were used to
- 16 capture GOM from the DFC sample lines while a Tekran® 2537A analyzer measured GEM
- 17 concurrently. Previous and ongoing work demonstrated that CEM do not collect GEM and
- 18 efficiently collects multiple compounds of GOM. Positive GOM emission rates up to 4000 pg m⁻
- 2 h⁻¹ were measured from tailings materials with high Hg substrate concentrations, and this has
- significant implication with respect to air-Hg surface exchange. GOM flux was variable for
- 21 lower Hg concentration substrates, with both emission and deposition observed, and this
- 22 was affected by ambient air GOM concentrations. For substrates that experienced GOM
- deposition, deposition velocities were in the range 0.01 0.07 cm s⁻¹.

Manuscript under review for journal Atmos. Meas. Tech.

Discussion started: 30 November 2018 © Author(s) 2018. CC BY 4.0 License.





25

26

27

28

29

30

31

32

33

34

35

36

37

38

39

40

41

42

43

44

45

46

1 Introduction

On 16 August 2017, the United Nations Environment Program (UNEP) Minamata Convention came into force with a mission to protect human health and the environment from exposure to the toxic effects of mercury (Hg) and its various compounds (UNEP, 2013). The Convention proposes to fulfill this mission through a strategy of globally coordinated scientific research, and ongoing monitoring of Hg in the environment where possible. The mission poses a significant challenge as there are over 3000 known Hg contaminated sites worldwide due to mining and industrial activity, not including legacy and small scale operations involving Hg (Kocman et al., 2013; Krabbenhoft and Sunderland, 2013). Past emissions were dominantly from natural sources, but are now largely from anthropogenic activities and have led to large reservoirs of Hg in all environmental compartments (Pacyna et al., 2016; Pirrone et al., 2010; Streets et al., 2017). Even in the absence of new anthropogenic emissions, cycling of Hg between different spheres will continue at large scales and in possibly unexpected directions, driven by processes and mechanisms that are not fully understood, and susceptible to increasing human and climate perturbations (Obrist et al., 2018). The atmosphere, a global common, is the dominant conduit for transport, transformation, emission, deposition, and re-emission of Hg and Hg compounds amongst Earth's ecosystems. Mercury in the atmosphere is classified on the basis of three physiochemical forms: gaseous elemental mercury (GEM), gaseous oxidized mercury (GOM), and particulate bound mercury (PBM), with PBM and GOM defined together as reactive mercury (RM = GOM + PBM)(Gustin et al., 2015). Atmospheric concentrations of GEM can be measured with well calibrated

Manuscript under review for journal Atmos. Meas. Tech.

Discussion started: 30 November 2018 © Author(s) 2018. CC BY 4.0 License.



47



analytical instruments, whereas the quantification of GOM and PBM has depended on 48 operationally defined methods with demonstrably large uncertainty (Cheng and Zhang, 2017; 49 Gustin et al., 2015; Gustin et al., 2013; Jaffe et al., 2014; Zhang et al., 2017). 50 Scientific understanding of the biogeochemical cycling of Hg is currently inadequate due to the large uncertainties in measurements, and general difficulty of research on atmospheric Hg 51 52 chemistry (Jaffe et al., 2014). Atmospheric GEM is relatively inert, has a low deposition rate, and hence a relatively long atmospheric lifetime ranging from minutes to 1 year (Krabbenhoft 53 and Sunderland, 2013; Zhang et al., 2009; Gustin et al., 2013). Observations of rapid depletion 54 55 of GEM from the atmosphere suggests that deposition and re-emission on short time scales is an 56 important process driving movement (Howard and Edwards, 2018; Lu et al., 2001; Schroeder et 57 al., 1998). In contrast to GEM, GOM compounds have higher dry deposition velocities (Zhang et 58 al., 2009). Knowledge of concentrations, chemistry, and processes forming atmospheric GOM is critical for understanding how Hg moves and impacts ecosystems globally. Recent research on 59 60 GOM has demonstrated that compounds in air vary both spatially and temporally to a 61 considerable extent, pointing to the need for extensive measurements of concentrations and 62 identifying the specific compounds (Gustin et al., 2016; Huang and Gustin, 2015b; Huang et al., 63 2014; Huang et al., 2017). 64 Fluxes of total gaseous mercury (TGM) and GEM have been successfully measured in many environments, providing insights into air-surface exchange that is critical for understanding 65 biogeochemical cycling of GEM (Yannick et al., 2016; Zhu et al., 2016). In contrast, there are 66 67 few direct measurements of GOM air-surface exchange (Zhang et al., 2009). GOM fluxes reported in the literature are largely based on measurements made with the KCl denuder as the 68

Manuscript under review for journal Atmos. Meas. Tech.

Discussion started: 30 November 2018 © Author(s) 2018. CC BY 4.0 License.



69



70 Castro et al., 2012; Engle et al., 2005; Lindberg et al., 2002; Lindberg and Stratton, 1998; Lyman 71 et al., 2009; Lyman et al., 2007; Malcolm and Keeler, 2002; Poissant et al., 2004; Rea et al., 72 2000; Rothenberg et al., 2010; Sather et al., 2013; Skov et al., 2006; Zhang et al., 2005; Huang et al., 2015b). The few direct GOM-specific air-surface exchange measurements using KCl 73 denuder-based approaches have been undertaken with mixed results (Brooks et al., 2008; Skov et 74 75 al., 2006). Moreover, recent evaluation of KCl denuder approaches show these methods tend to 76 underestimate GOM and are subject to interferences due to ozone and water vapor (Huang and Gustin, 2015a; Lyman et al., 2010; McClure et al., 2014). Understanding GOM air-surface 77 78 exchange processes would facilitate the Hg scientific community's ability to move forward in 79 understanding the biogeochemical cycling of atmospheric Hg. 80 In this study, we developed and applied a novel experimental approach for direct measurement 81 of GOM fluxes using cation exchange membrane (CEM) filters. CEM filters have been 82 successfully deployed to measure GOM in ambient air in previous studies (Gustin et al., 2016; 83 Huang et al., 2017; Huang et al., 2013; Marusczak et al., 2017; Pierce and Gustin, 2017), and 84 their use here was modified to allow for the determination of GOM air-surface exchange. A recent study (Miller et al., 2018) and ongoing work (unpublished data) have demonstrated that 85 86 GEM is not collected by the CEM and it efficiently collects a variety of GOM compounds. Here 87 is described a series of experiments that were conducted to optimize the CEM/GOM flux 88 methodology, and then, the resulting method was subsequently applied to determine fluxes over both background waste rock material and Hg enriched mining materials. Our research 89 hypothesis was the system developed would provide a means of determining if GOM is 90

GOM collection method, as well as a passive Hg dry deposition sampler (Brooks et al., 2008;

Manuscript under review for journal Atmos. Meas. Tech.

Discussion started: 30 November 2018 © Author(s) 2018. CC BY 4.0 License.





- 91 deposited or emitted from substrates, and this system would allow us to develop an
- 92 understanding of GOM air-surface exchange.

93 Methods

94

95

96

97

98

99

100

101

102

103

104

105

106

107

108

109

110

111

2.1 Materials

Substrate materials used for measuring Hg flux were acquired from industrial scale, open pit gold mines in central Nevada, and include waste rock, heap leach ore, and tailings. Materials were obtained from 4 ongoing mining operations: Twin Creeks (TC) and Lone Tree (LT) operated by Newmont Mining Corporation, and Cortez Pipeline (CP) and Gold Strike (GS) operated by Barrick Gold Corporation (Fig. 1; Table 1). There were 3 types of materials: waste rock called cap (C), heap leach material (L), and tailings (T or tails). (Waste rock is nonmineralized low Hg overburden consisting of alluvium or hard rock that covered the ore body prior to mining. For this study, materials were sampled from the waste rock piles specifically set aside for future capping and site reclamation, and as such is referred to as cap material. Heap leach is low-grade ore blasted from the mine wall and "heaped" on an impoundment for irrigation with dilute cyanide leach solution for gold extraction. Tailings are the waste remnant of high-grade ore that has been pulverized by mechanical ball milling and undergone thermal/chemical treatment to extract gold. All mining substrate materials were collected in September 2010, for measurements of GEM flux under controlled conditions (Miller and Gustin, 2013). Each material was divided into replicate trays (50 x 50 x 7 cm³ plywood lined with 3mil polyvinyl sheet) and stored inside a greenhouse bay at the University of Nevada Reno

Manuscript under review for journal Atmos. Meas. Tech.

Discussion started: 30 November 2018 © Author(s) 2018. CC BY 4.0 License.





paper, substrates were undisturbed for ~3 years, and were completely dry and well compacted/consolidated from previous watering experiments. A circular chamber footprint impression previously existed from prior experiments provided an excellent existing contact for the chamber base. Comparing GEM flux measurements made in this study with the previous measurements, an overall trend of decreasing GEM flux over time was observed. This fits a hypothesis suggested by Eckley et al. (2011b) of a long term reduction in GEM evasion from a mine substrate as time from disturbance increases.

2.2 Methodology

GOM flux was measured by modifying our existing GEM flux method consisting of a dynamic flux chamber (DFC) and an ambient air Hg analyzer (Tekran® 2537A) after the methods of

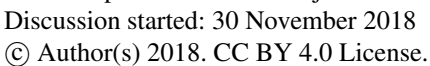
Agricultural Experiment Complex. At the onset of the GOM flux experiments described in this

Eckley et al. (2010; 2011a) and Miller et al. (2011).

Briefly, the GEM flux system used a 2537A in conjunction with a cylindrical DFC (footprint 0.036 m²) made of molded Teflon film (0.19 mm thick) over a rigid Teflon frame (1.5 mm thickness), with a total internal volume of 2.0 Liters (Fig. 2). Air enters the chamber through 24 inlet holes (1 cm diameter) spaced 2.5 cm apart around the perimeter and 2.0 cm above the bottom edge. The sample outlet is 0.625 cm diameter PTFE tubing at the top-center of the chamber, and sample inlet air is measured through equivalent tubing at the height of the chamber inlet holes. A Tekran® Automated Dual Switching (TADS) unit was used to cycle the sample flow (1.0 Lpm) between the chamber inlet and outlet lines in sequential 10 min intervals (two 5 min samples on each line). GEM in each 5 min sample volume was quantified automatically by the 2537A analyzer using pre-concentration on gold traps followed by thermal desorption (500

Manuscript under review for journal Atmos. Meas. Tech.

Discussion started: 30 November 2018





138

139

140

141

142

143

144

145

146

147

148

149

150

151

152

153

°C) and cold vapor atomic fluorescence spectrometry (CVAFS). The difference in Hg 134 concentration between the outlet and inlet air $(C_0 - C_1)$ referred to as ΔC , and was used to 135 136 calculate flux by Eq. 1:

137
$$F = Q * (C_0 - C_i)/A (1)$$

mean concentration of two consecutive 5 min outlet air samples (ng m⁻³), C_i is the mean concentration of inlet air in the samples before and after C₀, and A is the area of the substrate under the chamber (m^2). The sign of ΔC indicates the direction of flux with positive being emission and negative being deposition. The two modified systems included fitting the DFC inlet and outlet sample lines with 2-stage disc filter assemblies (Savillex[©] 47 mm PFA Teflon Filter Holder) holding two inline polysulfone cation exchange membranes (CEM 0.8 μm, Mustang® S, Pall Corporation) (Fig. 2). CEMs preferentially capture GOM compounds while allowing GEM to pass freely (Miller et al. 2018; unpublished data). The first upstream CEM served as the primary collection filter, while the second downstream CEM captured any Hg escaping from or missed by the first filter (referred to as breakthrough). With CEM filters deployed at the front of the sample lines, in conjunction with the 0.2 µm particulate filter at the rear sample inlet of the Tekran[®], GOM was scrubbed from the sample flow and all Hg measured downstream on the 2537A is in GEM form. An additional set of CEM filters was deployed simultaneously, using sample pumps and mass

flow controllers set to match the 2537A sample flow rate (1.0 Lpm, Fig. 2) at a height of 2 m

where F is the net Hg flux (ng m⁻² h⁻¹), Q is the flow rate through the chamber (m³ h⁻¹), C₀ is the

Manuscript under review for journal Atmos. Meas. Tech.

Discussion started: 30 November 2018 © Author(s) 2018. CC BY 4.0 License.





the greenhouse.

With both the Tekran® and external pump controlling CEM sample lines at 1 Lpm, total flow through the DFC was 2.0 Lpm that provides a chamber turn over time (TOT) of 1 minute. At this flow rate, flow velocity through the chamber is laminar with no turbulent eddy formation, as determined through computational fluid dynamic (CFD) modelling of the chamber geometry performed by Eckley et al. (2010). Thus the chamber design of Eckley et al. (2010) is optimal in

above the flux system. This was done to measure background ambient GOM concentrations in

particle entrainment from the substrate surfaces is not expected, especially for particle sizes

terms of not disturbing the substrate being studied. With low velocity, non-turbulent flow,

greater than the CEM filter pore size of 0.8 µm.

2.3 Analyses

After flux measurements, CEM filters were collected into sterile 50 mL polypropylene centrifuge tubes, and frozen at -20 °C until analyses (within 14 days of collection). Filters were analyzed for total Hg by aqueous digestion and cold vapor atomic fluorescence spectrometry (CVAFS, EPA Method 1631, Rev. E) using a Tekran 2600 system, with total Hg operationally equivalent to total GOM. The blank Hg mass that can be expected on an unused CEM filter (median = 68 pg, n = 56) was determined from clean filters collected with every set of measurements, and the median blank value was subtracted from all sample values. Breakthrough is defined as the amount of Hg on the secondary filter as a percent of the total Hg collected on both filters (after blank correction), and overall median breakthrough was low (4.2%, n = 222).

Manuscript under review for journal Atmos. Meas. Tech.

Discussion started: 30 November 2018 © Author(s) 2018. CC BY 4.0 License.



174



corrected primary and secondary filters into a total Hg mass per sample line and dividing by the 175 176 respective sample air volume. The difference in GOM concentration between the inlet and outlet 177 lines provided a ΔC_{GOM} , with this multiplied by sample flow providing the GOM emission rate (pg h⁻¹). Reactive Hg flux (pg m⁻² h⁻¹) was calculated with Eq. 1 using ΔC_{GOM} values, the flow 178 179 rate $(1.0 \pm 0.005 \text{ Lpm})$ and the chamber footprint (0.036 m^2) . The GOM flux detection limit was determined by the minimum statistically resolvable difference 180 between C_0 and C_i , i.e. the smallest meaningful ΔC_{GOM} that could be measured (Fig. 3). The C_0 181 and Ci concentrations were based on two measurements: total Hg on the CEM filters as 182 determined by analysis on the Tekran[®] 2600 system, and total sample volume as determined by 183 184 the mass flow-controlled sample rate and time. The MFC precision was $\pm 0.5\%$ (± 0.005 Lpm at 185 1.0 Lpm) and the detection limit of the 2600 was 1 ppt, or \sim 53 pg per reagent blank in a clean 50 mL collection tube. The median mass of Hg on the blank CEM filters was 68 pg and was used as 186 the practical detection limit for the method. As the distribution of CEM blank values was non-187 188 normal and skewed heavily to the right (Fig. 3a), the 95% confidence interval around the median (58 – 73 pg) was used to define a minimum detectable GOM concentration (Fig. 3b). For 189 example, in a 24 h sample, the minimum detectable GOM concentration would be ~ 3.5 pg m⁻³ to 190 exceed the upper 95% confidence limit of 73 pg. In a 24 h sample the minimum resolvable 191 ΔC_{GOM} would be 13.5 pg m⁻³ (sum of upper + lower confidence intervals, + 3 pg m⁻³ to account 192 193 for flow precision, converted to 24 h sample volume concentration). This was taken as the upper 194 minimum ΔC_{GOM} value.

The GOM concentration in the inlet/outlet sample air was calculated by combining the blank-

Manuscript under review for journal Atmos. Meas. Tech.

Discussion started: 30 November 2018 © Author(s) 2018. CC BY 4.0 License.





Chamber blanks were determined for each Teflon DFC (referred to as Chamber A and Chamber B) by measuring flux over a clean Teflon sheet. Chamber blank emission rates were measured immediately following chamber cleanings (24 h acid wash, 10% HNO₃), and then between substrate types (i.e. cap, leach, tailings). For the summer measurement period, the median chamber blank Δ CGOM for both Chambers A and B (A = 13 pg m⁻³, B = 14 pg m⁻³, n = 12) was at the detection limit, so chamber blanks were not subtracted from material fluxes. This was due to high ambient GOM concentrations in the greenhouse. For the following winter measurement period, the median chamber blank Δ CGOM for both chambers was significantly negative (A = -60 pg m⁻³, B= -60 pg m⁻³, n = 6), and the median chamber blank was -215 pg m⁻² h⁻¹, indicating that the chamber and the blank Teflon sheet were acting as depositional surfaces for GOM. For these measurements, the chamber blanks were subtracted. For materials that demonstrated net GOM deposition, the deposition velocity (V_d cm s⁻¹) was calculated using Eq. 2:

207
$$V_d = \text{flux} (ng \, m^{-2} \, h^{-1}) / \text{air concentration} (ng \, m^{-3}) * (100/3600)(2)$$

All fluxes were measured in the University of Nevada-Reno Agricultural Experiment Station greenhouse. Meteorological parameters were measured synchronously with flux and recorded in 5 min averages, including temperature and relative humidity (HMP45C, Campbell Scientific®), substrate temperature (C107, Campbell Scientific®), and solar radiation (LI-200X, LiCor®). Rudimentary climate control was provided by ventilation fans pulling outside air across the greenhouse bay from intakes on the opposite side. Fluxes were measured on the "upwind" side of the bay in a variety of orientations (see below).

Data was processed in Microsoft Excel (version 16.22) and RStudio[®] (version 3.2.2).

Manuscript under review for journal Atmos. Meas. Tech.

Discussion started: 30 November 2018 © Author(s) 2018. CC BY 4.0 License.





2.4 Development of the method

Two Tekran® 2537A analyzers with associated GOM filter systems were used to simultaneously measure flux from two replicate trays (one for each A and B system) of each sample material. The duplicated systems allowed a total of four GOM flux measurements to be collected each time a material was tested, two from the Tekran® sample lines and two from the external pump lines. The intention of the duplicate systems was to evaluate consistency and repeatability of the measurements. However, during the initial method testing it became apparent that the position of the trays and the inlet sample lines was an important variable. For example, strong GOM emission from an "upwind" tray could substantially increase the inlet GOM concentration of the "downwind" tray, resulting in a negative ΔC_{GOM} and apparent deposition. Such contradictory results compelled us to test a variety of orientations for the two systems. The best results were achieved in the final design by placing both trays all the way against the intake wall of the greenhouse bay, and separating them laterally by 1.5 m, with all equipment located downwind. This configuration provided the most uniform inlet air concentrations for both systems.

2.5 Limitations of method

The use of filter membranes in conjunction with a DFC to measure GOM flux has several limitations. Given the low concentrations of GOM, a relatively long sampling time of at least 24 h is required to capture a sufficient mass for quantification on low Hg containing substrates.

Despite the limitations, this method moves us a step further for understanding GOM flux. The low temporal resolution limits analysis of the factors controlling GOM flux, since there will be changes on a diel cycle similar to observations of GEM flux (c.f. Gustin et al., 2013). In

Manuscript under review for journal Atmos. Meas. Tech.

Discussion started: 30 November 2018 © Author(s) 2018. CC BY 4.0 License.





237 addition, flow rate and surface area could be increased, but in order to change this method a number of proof of concept tests would have to be done. 238 239 A necessary condition of the DFC method is the placement of flux chambers directly on a 240 material, resulting in artificial modification of surface conditions and a presumptive influence on the magnitude of flux. In our study, this limitation is immaterial, as the entire experimental setup 241 242 constitutes an artificial environment, and we are more interested in 1) our ability to experimentally detect measurable GOM flux, and 2) the qualitative direction of flux versus 243 244 absolute quantification. As the method develops, it will become necessary to more thoroughly 245 evaluate the effects of the DFC on GOM flux. Lastly, CEM were analyzed within two weeks of collection. Pierce et al. (2017) demonstrated 246 247 that little HgCl₂ was lost from the membranes over this time period. This needs to be tested for 248 other GOM compounds thought to be present in the atmosphere (Huang et al., 2013; Gustin et 249 al., 2016). 250 3 Results 251 3.1 GOM flux measurement repeatability The first test of the optimized configuration was a set of replicate measurements made on a 252 253 single material, to assess method repeatability. The material used for this test was a heap leach ore of intermediate total Hg concentration (TCL, $13.2 \pm 2.0 \,\mu g \,g^{-1}$). Filters were deployed in 254 three consecutive sample sets of approximately 72 h each, for a total of 12 replicate filter flux 255 256 measurements (i.e. two GOM flux measurements on two separate replicate trays, three times). The mean GEM flux from all samples was 167 ± 57 ng m⁻² h⁻¹ (n = 6). The duplicate 257

Manuscript under review for journal Atmos. Meas. Tech.

Discussion started: 30 November 2018 © Author(s) 2018. CC BY 4.0 License.





measurements of background greenhouse GOM showed a mean concentration of 13 ± 7 pg m⁻³ 258 (n = 12). The ΔC_{GOM} was well above detection for all measurements (median 97 pg m⁻³, n = 12), 259 and the mean GOM flux over all 12 samples was 370 \pm 80 pg m⁻² h⁻¹ (n = 12) and ranged from 260 240 to 490 pg m⁻² h⁻¹ (Fig. 4). 261 262 The mean relative percent difference (RPD) of GOM flux measured between Pump and Tekran sample lines on the same tray was $6.5 \pm 3.9\%$, and mean RPD between trays was 21.4%. These 263 264 replicate measurements of a single material consistently showed the same direction and magnitude of GOM flux with good agreement. 265 266 3.2 GOM flux measurement replication over expanded range of materials: Summer 267 Following the triplicate measurement of TCL (May), follow up testing was conducted on a series of three additional materials (July - August): a low to intermediate Hg cap material and heap 268 leach ore (TCC 0.2 µg g⁻¹, LTL 0.6 µg g⁻¹), and a high Hg tailings (TCT 36 µg g⁻¹). 269 270 Measurement time was reduced to 48 h for this series of materials, as the previous deployments 271 had total GOM loading well above detection. However, several of the LTL and TCC flux 272 measurements resulted in insignificant ΔC_{GOM} values (Fig. 5). In these cases, GOM flux could 273 not be discriminated, and these values were excluded from subsequent analysis. 274 A comparison of GOM flux measured by the replicate sample lines on each system (Tekran® 275 sample flow and external pump sample flow) show a relationship of 1:1 (Fig. 6) that indicates 276 that CEM filters on two independent flow channels were capturing equivalent amounts of GOM. This equivalency was true for both of the replicate systems (System A and B) that were each 277 simultaneously measuring flux from replicate trays of the same material. The high level of 278

Manuscript under review for journal Atmos. Meas. Tech.

Discussion started: 30 November 2018 © Author(s) 2018. CC BY 4.0 License.



279



replication displayed by the system, both in general and in detail, for multiple substrate types, 280 increases confidence that these measurements represent a real net surface exchange of GOM. 281 Positive GOM fluxes were associated with the higher substrate concentration materials (TCL, 282 TCT). The low Hg TCC experienced net GOM deposition, with a mean V_d of 0.03 ± 0.01 cm s⁻¹ 283 (n = 6). The 3x higher Hg concentration LTL showed either no net flux or slightly positive GOM emission ($64 \pm 10 \text{ pg m}^{-2} \text{ h}^{-1}$, n = 3). The very high substrate Hg concentration TCT materials 284 showed uniformly high GOM emission ($4060 \pm 1000 \text{ pg m}^{-2} \text{ h}^{-1}, \text{ n} = 7$). 285 The mean ambient GOM in the greenhouse during this period was 130 ± 55 pg m⁻³ (n = 24); 286 287 however, there was a distinct trend of increasing ambient GOM over the course of measurements. During the TCC measurements, ambient GOM concentration in the greenhouse 288 was 70 ± 20 pg m⁻³ (n = 8). This increased to 150 ± 20 pg m⁻³ (n = 8) during the LTL 289 measurements, and up to 180 ± 40 pg m⁻³ (n = 8) during the TCT measurement. 290 3.3 GOM flux measurement over complete range of materials: Winter 291 292 A full set of 24 h GOM flux measurements including all the available mining materials was 293 made in the following winter period (January – March, 2016). Ambient GOM concentration in greenhouse air was 50 pg m^{-3} (n = 16), much lower than in the summer months. Mean RH and 294 295 solar radiation were similar between the summer and winter periods, due to the attenuating effect 296 of the greenhouse. However, mean air and substrate temperatures were significantly lower in the 297 winter (Table 1). 298 All measured fluxes were above the ΔC_{GOM} detection limit (Fig. 7a). The relationship between 299 GOM flux measured on the A and B systems was slightly less than 1:1 (B = 0.87*A) and not as

Manuscript under review for journal Atmos. Meas. Tech.

Discussion started: 30 November 2018 © Author(s) 2018. CC BY 4.0 License.





strong $(r^2 = 0.74)$ as during the summer measurements. Without chamber blank correction, GOM 300 fluxes were uniformly negative for all materials except the very high Hg TCT (Fig. 7b, orange 301 302 shades). However, with the chamber blank correction applied, GOM flux from the cap materials 303 became ambiguous (i.e. both deposition and emission observed) and positive for all leach and 304 tailings materials except the LTT (Fig. 7c, green shades). Three replicated materials had consistent fluxes, with or without blank correction: GS cap (GOM 305 deposition, $V_d = 0.02 - 0.04$ cm s⁻¹, corrected), LTT (GOM deposition, $V_d = 0.01 - 0.05$ cm s⁻¹, 306 corrected), and TCT (strong GOM emission). The GS mine exploits a predominantly 307 carbonaceous ore deposit, and much of the mine and surrounding areas are subject to carbon 308 loading from aerial dust deposition. The carbon in the GS waste rock and ore likely facilitate 309 310 deposition of Hg and GOM (c.f. Miller et al, 2013; Eckley et al., 2011), . The LTT material is 311 from a non-active tailings impoundment that was partially revegetated at the time of collection, versus the entirely barren surface typical of active tailings. Although the LTT Hg concentration 312 was high (11 μg g⁻¹), the surface was old, and it is possible this material behaved more as a 313 background substrate. The TCT material was collected from an actively filling tailings 314 impoundment that collected process waste from a variety of ore types, from multiple mine sites, 315 316 and had the highest Hg concentration of the materials used in this study, which likely explains its 317 tendency to by a strong emitter of both GEM and GOM, a conclusion also made by Eckley et al. 318 (2011a). An interesting point is that background (2 m and inlet GOM concentrations were very similar 319 during the summer measurements (Fig. 8a), but inlet concentrations were 3x higher than 320 background during the winter measurements (Fig. 8b). The lower winter background GOM (50 321

Manuscript under review for journal Atmos. Meas. Tech.

Discussion started: 30 November 2018 © Author(s) 2018. CC BY 4.0 License.





pg m⁻³) compared to summer (110 pg m⁻³) may partially explain this, however the distance between the inlet and background sampling heights was only ~ 1 m, which implies a strong vertical gradient in GOM concentration in the greenhouse air. The explanation for this is less well mixed air in the greenhouse bay during the winter, as the greenhouse circulation was shut down at temperatures approaching 13 °C, setting up stratified conditions. The relatively high inlet level GOM concentrations during the winter also caused the higher deposition observed in the chamber blank measurements during this time.

4 Conclusions

This study presents direct GOM flux measurements using a CEM filter technique and provides an analysis of whether the necessary measurements of small differences in GOM concentration were possible using a DFC method. Measurements of GOM flux were above calculated detection limits in most cases, and both intra- (Tekran vs Pump sample) and inter- (A vs B) system replicate measurements showed very good agreement. After initial trials at 72 h and 48 h, a 24 h sample time was found to be generally sufficient for detecting GOM flux on the mining materials used in this study, some of which were similar to background soils. It would be possible to operate the system at higher flow rates, to decrease sample time and improve the temporal resolution of the flux measurements. However, sample deployment and collection require 20-30 min and to some extent perturbs the system, so ultimately the flux resolution is limited by practical operational constraints. The 24 h measurement at least serves to capture net flux over a full diel cycle without continuous interruptions.

We specifically refer to our measurement as GOM. This is because particulate Hg is not *emitted* from a surface in the volatile sense, and particle entrainment was negligible at the low flow

Manuscript under review for journal Atmos. Meas. Tech.

Discussion started: 30 November 2018 © Author(s) 2018. CC BY 4.0 License.





velocities generated in the flux chambers. Thus GOM concentrations measured at the chamber 344 outlet CEM filters are dominated by GOM. If ambient air GOM concentrations were primarily 345 PBM, at a size fraction large enough to be captured by the CEM filters (i.e. $> 0.8 \mu m$), it will 346 347 undeniably be captured at the chamber inlet filters. However, PBM at this size would likely 348 deposit to the substrate surface within the chamber, thus deposition is GOM loading on the C₀ 349 filters versus the Ci filters. Here we have demonstrated that GOM can be deposited and emitted from a surface. It is unlikely 350 GOM was produced by oxidation of GEM given short time of air moving through the chamber 351 352 and the fact that strong oxidants were likely removed as air moved through air handlers into the greenhouse. This is a unique scientific finding. Flux measured from low Hg, non-mineralized 353 354 cap materials for both GEM and GOM were low positive and negative values oscillating around 355 a net zero flux (Table 1). The observed GEM deposition velocities were typical of non-vegetated surfaces, while GOM deposition occurred at V_d values (0.01 – 0.07 cm s⁻¹) on the low end of the 356 357 suggested range (Zhang et al., 2009). The higher Hg concentration leach and tailings material (except LT tails) showed net GEM and GOM emission in the summer, while deposition was 358 observed for both for most materials in the winter. The highest GOM emissions were 359 360 consistently observed for the highest Hg concentration substrate, TCT, in both summer and 361 winter conditions with fluxes higher in the summer during which time the greenhouse was better 362 mixed. The implications of these results are that GOM fluxes may be directly measured and that contaminated areas such as mine tailings impoundments can act as a direct emission source of 363 364 GOM compounds to the atmosphere.

365 366

Acknowledgements

Manuscript under review for journal Atmos. Meas. Tech.

Discussion started: 30 November 2018 © Author(s) 2018. CC BY 4.0 License.



367



368 629679, Barrick Gold Corp and Newmont Mining Corp for donating substrate materials, and Dr. 369 Ashley Pierce for invaluable assistance in preparing this manuscript. 370 371 372 References 373 Brooks, S., Arimoto, R., Lindberg, S., and Southworth, G.: Antarctic polar plateau snow surface 374 conversion of deposited oxidized mercury to gaseous elemental mercury with fractional 375 long-teGOM burial, Atmospheric Environment, 42, 2877-2884, 2008. 376 Castro, M. S., Moore, C., Sherwell, J., and Brooks, S. B.: Dry deposition of gaseous oxidized 377 mercury in Western Maryland, Science of the Total Environment, 417-418, 232-40, 2012. 378 Cheng, I., and Zhang, L.: Uncertainty Assessment of Gaseous Oxidized Mercury Measurements 379 Collected by Atmospheric Mercury Network, Environmental Science & Technology, 51, 380 855-862, 2017. 381 Eckley, C. S., Gustin, M., Lin, C. J., Li, X., and Miller, M. B.: The influence of dynamic 382 chamber design and operating parameters on calculated surface-to-air mercury fluxes, Atmospheric Environment, 44, 194-203, 2010. 383 Eckley, C.S., Gustin, M., Marsik, F., and Miller, M.B.: Measurement of surface mercury fluxes 384 at active industrial gold mines in Nevada (USA), Science of the Total Environment, 409, 385 386 514-522, 2011a. 387 Eckley, C. S., Gustin, M., Miller, M.B., and Marsik, F.: Scaling Non-Point-Source Mercury 388 Emissions from Two Active Industrial Gold Mines: Influential Variables and Annual Emission Estimates, Environmental Science & Technology, 45, 392-399, 2011b. 389 390 Engle, M. A., Sexauer Gustin M, Lindberg, S. E., Gertler, A.W., and Ariya, P.A.: The influence of ozone on atmospheric emissions of gaseous elemental mercury and reactive gaseous 391 mercury from substrates, Atmospheric Environment, 39, 7506-7517, 2005... 392 Gustin, M. S., Amos, H.M., Huang, J., Miller, M.B., and Heidecorn, K.: Measuring and 393 modeling mercury in the atmosphere: a critical review, Atmos. Chem. Phys. 15: 5697-394 5713, 2015. 395 Gustin, M. S., Huang, J., Miller, M. B, Peterson C., Jaffe, D. A., Ambrose, J, et al.: Do We 396 397 Understand What the Mercury Speciation Instruments Are Actually Measuring? Results of RAMIX, Environmental Science & Technology, 47, 7295-7306, 2013. 398

The authors would like to acknowledge funding from National Science Foundation Grant

Manuscript under review for journal Atmos. Meas. Tech.

Discussion started: 30 November 2018 © Author(s) 2018. CC BY 4.0 License.



399



400 401 402	Evidence for Different Reactive Hg Sources and Chemical Compounds at Adjacent Valley and High Elevation Locations, Environmental Science & Technology, 50, 12225-12231, 2016.
403 404 405	Howard, D., and Edwards, G.C.: Mercury fluxes over an Australian alpine grassland and observation of nocturnal atmospheric mercury depletion events, Atmos. Chem. Phys., 18, 129-142, 2018.
406 407 408	Huang, J. and Gustin, M.S.: Uncertainties of Gaseous Oxidized Mercury Measurements Using KCl-Coated Denuders, Cation-Exchange Membranes, and Nylon Membranes: Humidity Influences, Environmental Science & Technology, 49, 6102-6108, 2015a.
409 410 411	Huang, J. and Gustin, M.S.: Use of Passive Sampling Methods and Models to Understand Sources of Mercury Deposition to High Elevation Sites in the Western United States; Environmental Science & Technology, 49, 432-441, 2015b.
412 413 414	Huang, J., Lyman, S.N., Hartman, J.S., and Gustin, M.S.: A review of passive sampling systems for ambient air mercury measurements, Environmental Science: Processes & Impacts 16: 374-392, 2014.
415 416 417	Huang, J., Miller, M.B., Edgerton, E., and Sexauer Gustin, M. Deciphering potential chemical compounds of gaseous oxidized mercury in Florida, USA, Atmos. Chem. Phys., 17, 1689-1698, 2017.
418 419 420	Huang, J., Miller, M.B., Weiss-Penzias, P., and Gustin, M.S.: Comparison of Gaseous Oxidized Hg Measured by KCl-Coated Denuders, and Nylon and Cation Exchange Membranes, Environmental Science & Technology, 47, 7307-7316, 2013.
421 422 423	Jaffe, D. A., Lyman, S., Amos, H.M., Gustin, M. S., Huang, J., Selin, N.E., et al.: Progress on Understanding Atmospheric Mercury Hampered by Uncertain Measurements. Environmental Science & Technology, 48, 7204-7206, 2014.
424 425	Kocman, D., Horvat, M., Pirrone, N., and Cinnirella, S.: Contribution of contaminated sites to the global mercury budget. Environmental Research, 125, 160-170, 2013.
426 427	Krabbenhoft, D.P. and Sunderland E. M.: Global Change and Mercury, Science, 341, 1457, 2013.
428 429 430	Lindberg, S.E., Brooks, S., Lin, C.J., Scott, K. J., Landis, M.S., Stevens, R.K., et al.: Dynamic Oxidation of Gaseous Mercury in the Arctic Troposphere at Polar Sunrise; Environmental Science & Technology, 36, 1245-1256, 2013.
431 432 433	Lindberg, S.E., and Stratton, W.J.: Atmospheric mercury speciation: Concentrations and behavior of reactive gaseous mercury in ambient air, Environmental Science & Technology 32: 49-57.

Gustin, M. S., Pierce, A.M., Huang, J., Miller, M.B., Holmes, H.A., and Loria-Salazar, S.M.:

Manuscript under review for journal Atmos. Meas. Tech.

Discussion started: 30 November 2018 © Author(s) 2018. CC BY 4.0 License.





434 Lu, J., Schroeder, W., Barrie, L., Steffen, A., Welch, H., Martin, K., et al.: Magnification of 435 atmospheric mercury deposition to polar regions in springtime: the link to tropospheric 436 ozone depletion chemistry, Geophysical Research Letters, 28, 3219-3222, 2001. 437 Lyman, S.N, Gustin, M. S., Prestbo, E. M., Kilner, P. I., Edgerton, E., Hartsell, B.: Testing and 438 Application of Surrogate Surfaces for Understanding Potential Gaseous Oxidized Mercury Dry Deposition, Environmental Science & Technology, 43, 6235-6241, 2009. 439 440 Lyman, S.N., Gustin, M. S., Prestbo, E.M., and Marsik, F.J.: Estimation of Dry Deposition of 441 Atmospheric Mercury in Nevada by Direct and Indirect Methods, Environmental Science 442 & Technology, 41, 1970-1976, 2007. 443 Lyman, S.N., Jaffe, D. A., and Gustin, M.S.: Release of mercury halides from KCl denuders in 444 the presence of ozone, Atmospheric Chemistry and Physics, 10, 8197-8204, 2010. 445 Malcolm, E.G., and Keeler, G.J.: Measurements of mercury in dew: atmospheric removal of 446 mercury species to a wetted surface, Environmental Science & Technology, 36, 2815-447 2821, 2002. 448 Marusczak N, Sonke JE, Fu X, Jiskra M. Tropospheric GOM at the Pic du Midi Observatory— Correcting Bias in Denuder Based Observations. Environmental Science & Technology 449 450 2017; 51: 863-869. 451 McClure, C. D., Jaffe, D.A., and Edgerton, E.S.: Evaluation of the KCI Denuder Method for 452 Gaseous Oxidized Mercury using HgBr2 at an In-Service AMNet Site, Environmental Science & Technology, 48, 11437-11444, 2014. 453 Miller, M.B. and Gustin, M.S.: Testing and modeling the influence of reclamation and control 454 methods for reducing nonpoint mercury emissions associated with industrial open pit 455 456 gold mines, Journal of the Air & Waste Management Association, 63, 681-693, 2013. 457 Miller, M.B., Gustin, M.S., and Eckley, C.S.: Measurement and scaling of air-surface mercury 458 exchange from substrates in the vicinity of two Nevada gold mines, Science of the Total Environment, 409, 3879-3886, 2011. 459 460 Miller, M.B., Gustin, M. S., Dunham-Cheatham, S.S., and Edwards, G.C 2018 Evaluation of cation exchange membrane performance under exposure to high Hg⁰ and 461 HgBr2 concentrations Atmospheric Measurement Techniques 462 https://doi.org/10.5194/amt-2018-127, 2018 463 464 465 Obrist, D., Kirk, J., Zhang, L., Sunderland, E., Jiskra, M., Selin, N.: A review of global 466 environmental mercury processes in response to human and natural perturbations: Changes of emissions, climate, and land use, Ambio, 47, 116-140 2018. 467 Pacyna, J., Travnikov, O., De Simone, F., Hedgecock, I., Sundseth, K., Pacyna, E, et al.: Current 468 469 and future levels of mercury atmospheric pollution on a global scale. Atmospheric Chemistry and Physics; 16, 12495-12511, 2016. 470

Manuscript under review for journal Atmos. Meas. Tech.

Discussion started: 30 November 2018 © Author(s) 2018. CC BY 4.0 License.



471



Pierce, A.M., and Gustin, M.S.: Development of a Particulate Mass Measurement System for 472 Quantification of Ambient Reactive Mercury, Environmental Science & Technology 51: 473 436-445, 2017. 474 Pirrone, N., Cinnirella, S., Feng, X., Finkelman, R., Friedli, H., Leaner, J. et al.: Global mercury 475 emissions to the atmosphere from anthropogenic and natural sources, Atmospheric Chemistry and Physics, 10, 5951-5964, 2010. 476 477 Poissant, L., Pilote, M., Xu, X., Zhang, H., and Beauvais, C.: Atmospheric mercury speciation 478 and deposition in the Bay St. Francois wetlands, Journal of Geophysical Research-479 Atmospheres, 109, D11, D11301 **DOI**: 10.1029/2003JD004364 480 481 Rea, A.W., Lindberg, S.E., and Keeler, G.J.: Assessment of Dry Deposition and Foliar Leaching 482 of Mercury and Selected Trace Elements Based on Washed Foliar and Surrogate 483 Surfaces, Environmental Science & Technology, 34, 2418-2425, 2000. 484 Rothenberg, S.E., McKee, L., Gilbreath, A., Yee, D., Connor, M., and Fu, X.: Evidence for short-range transport of atmospheric mercury to a rural, inland site, Atmospheric 485 486 Environment, 44, 1263-1273, 2010. 487 Sather, M. E., Mukerjee, S., Smith, L., Mathew, J., Jackson, C., Callison, R., et al.: Gaseous 488 oxidized mercury dry deposition measurements in the Four Corners area and Eastern Oklahoma, U.S.A, Atmospheric Pollution Research, 4, 168-180, 2013. 489 490 Schroeder, W.H., Anlauf, K.G., Barrie, L.A., Lu, J.Y., Steffen, A., Schneeberger, D. R., et al.: 491 Arctic springtime depletion of mercury, Nature, 394, 331, 1998. 492 Skov, H., Brooks, S.B., Goodsite. M.E., Lindberg, S.E., Meyers, T.P., Landis, M. S., et al.: 493 Fluxes of reactive gaseous mercury measured with a newly developed method using 494 relaxed eddy accumulation, Atmospheric Environment, 40, 5452-5463, 2006. 495 Streets, D. G., Horowitz, H. M., Jacob, D. J., Lu, Z., Levin, L., ter Schure, A.F.H., et al. Total 496 Mercury Released to the Environment by Human Activities. Environmental Science & Technology 51, 5969-5977, 2017. 497 498 UNEP. Minamata Convention on Mercury, 2013. 499 Yannick, A., Théo, Le D., Christopher, W. M., Grant, C. E., and Obrist, D.: New Constraints on 500 Terrestrial Surface-Atmosphere Fluxes of Gaseous Elemental Mercury Using a Global Database, Environmental Science & Technology, 50, 507-524, 2016. 501 502 Zhang, H. H., Poissant, L., Xu, X., and Pilote, M.: Explorative and innovative dynamic flux bag method development and testing for mercury air-vegetation gas exchange fluxes, 503 504 Atmospheric Environment, 39, 7481-7493, 2005.

Atmos. Meas. Tech. Discuss., https://doi.org/10.5194/amt-2018-360 Manuscript under review for journal Atmos. Meas. Tech.

Discussion started: 30 November 2018 © Author(s) 2018. CC BY 4.0 License.





Zhang, L., Lyman, S., Mao, H., Lin, C., Gay, D., Wang, S., et al.: A synthesis of research needs
 for improving the understanding of atmospheric mercury cycling, Atmospheric
 Chemistry and Physics, 17, 9133-9144, 2017.

Zhang, L. M., Wright, L.P., and Blanchard, P.: A review of current knowledge concerning dry deposition of atmospheric mercury, Atmospheric Environment, 43, 5853-5864, 2009.

Zhu, W., Lin, C., Wang, X., Sommar, J., Fu, X., and Feng, X.: Global observations and modeling of atmosphere-surface exchange of elemental mercury: a critical review, Atmospheric Chemistry and Physics, 16, 4451-4480, 2016.

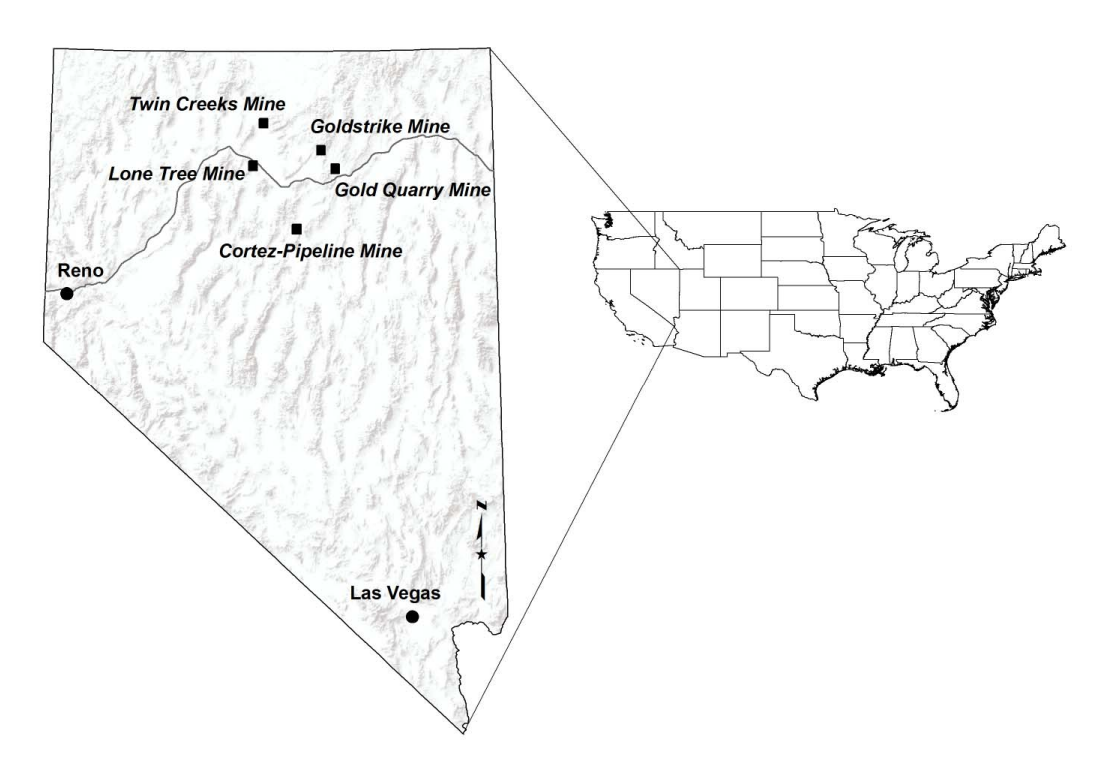


Figure 1. Location map of study sites, Nevada, USA (From Miller and Gustin, 2013).

Atmos. Meas. Tech. Discuss., https://doi.org/10.5194/amt-2018-360 Manuscript under review for journal Atmos. Meas. Tech.

Discussion started: 30 November 2018 © Author(s) 2018. CC BY 4.0 License.





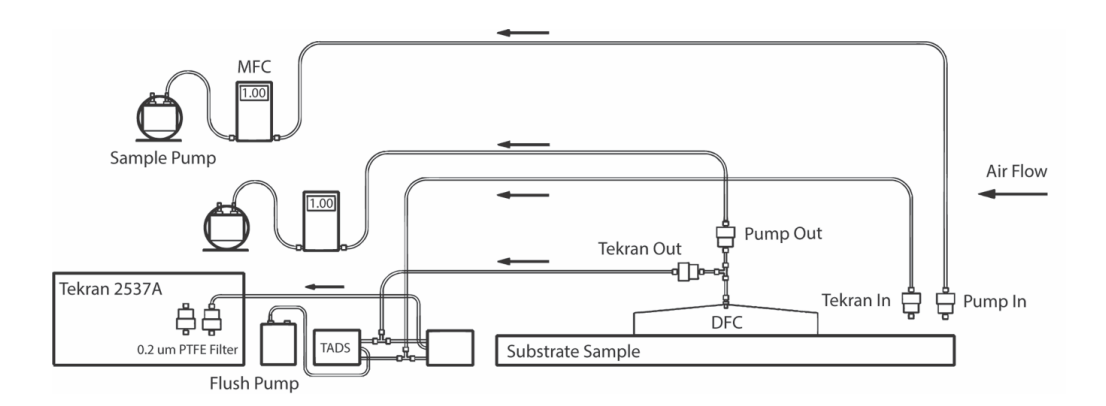


Figure 2. Diagram of one GOM filter-based flux system, deployed in duplicate as Systems A and B..Filter packs indicate the location of the CEM samples.

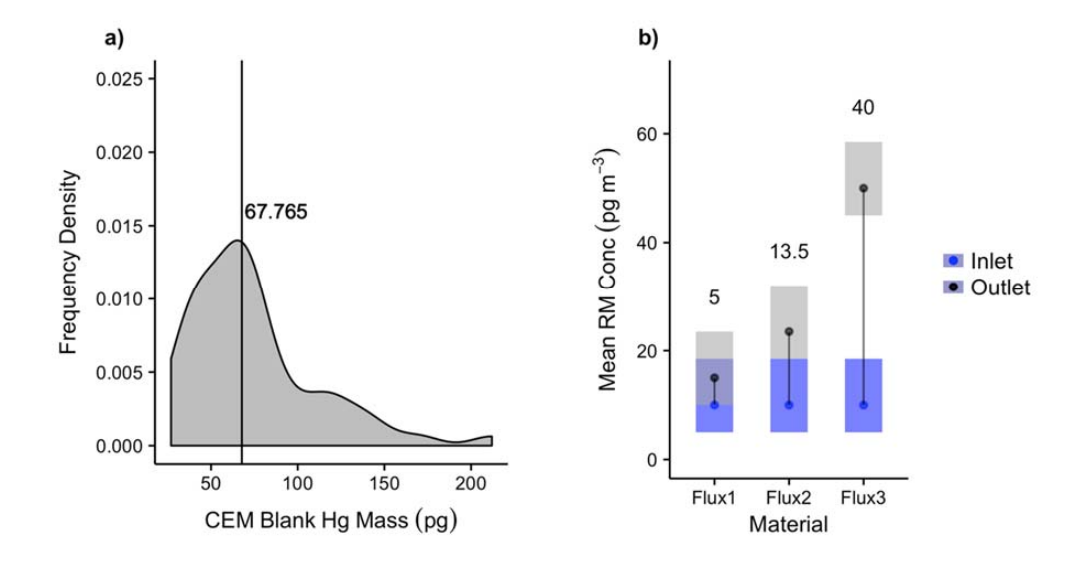


Figure 3. Determination of ΔC_{GOM} detection limit. a) Distribution of Hg mass on unused "blank" CEM filters (median = 68 pg) b) Hypothetical example of statistically detectable GOM flux criteria: shaded boxes represent the maximum uncertainty in concentration, based on 95% confidence interval around the median filter blank (58 – 73 pg), Flux1 represents an insufficiently resolvable ΔC_{GOM} in which the 95% confidence intervals around the median blank-corrected C_o and C_i values overlap, Flux2 represents the minimum detectable ΔC_{GOM} (13.5 pg m⁻³), and Flux3 represents an obviously resolvable ΔC_{GOM} .

Atmos. Meas. Tech. Discuss., https://doi.org/10.5194/amt-2018-360 Manuscript under review for journal Atmos. Meas. Tech.

Discussion started: 30 November 2018 © Author(s) 2018. CC BY 4.0 License.





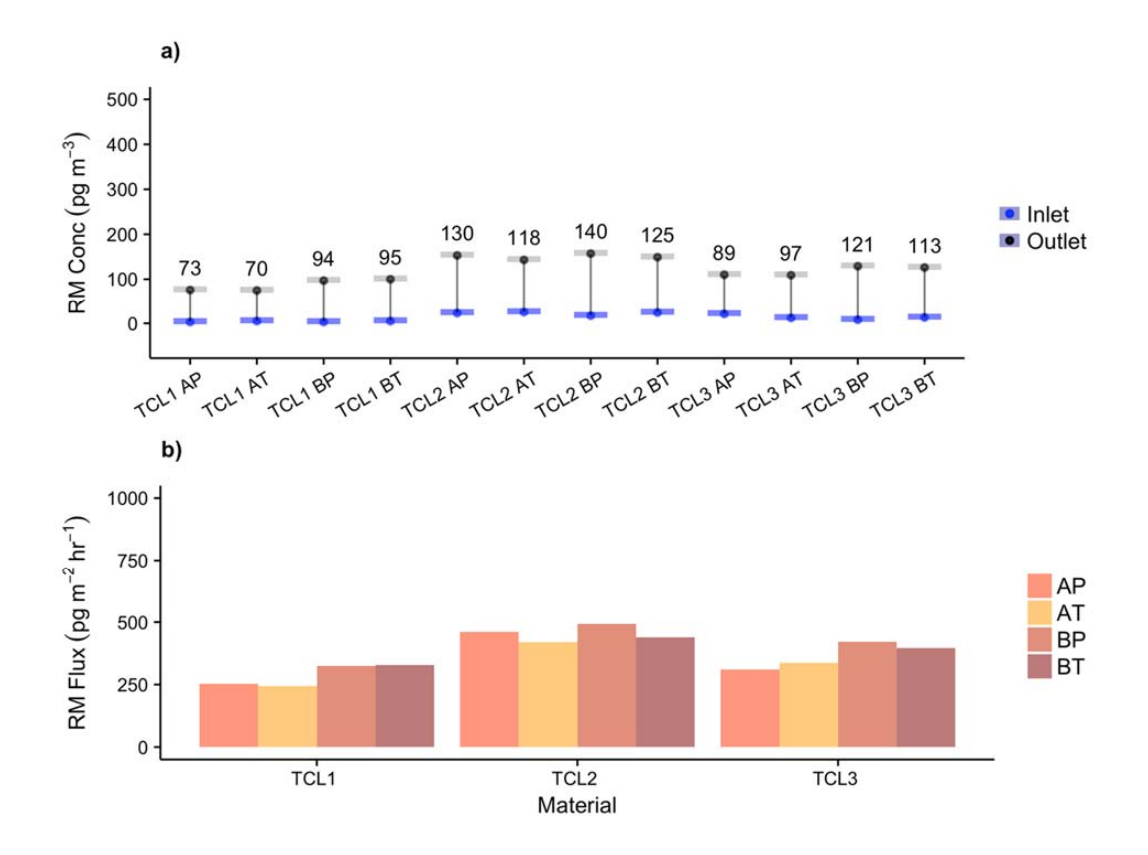


Figure 4. Test 72 h replicate measurements of TCL material. a) ΔC_{GOM} values: grey points indicate chamber concentration (C_o), blue points indicate inlet air concentration (C_i), and the numeric value of ΔC_{GOM} is shown above b) GOM flux from TCL material in three consecutive 72 h measurements, no chamber blank correction. Sample line labels: AP = Pump A,PB = Pump B, AT = Tekran A, BT = Tekran B.

Atmos. Meas. Tech. Discuss., https://doi.org/10.5194/amt-2018-360 Manuscript under review for journal Atmos. Meas. Tech.

Discussion started: 30 November 2018 © Author(s) 2018. CC BY 4.0 License.





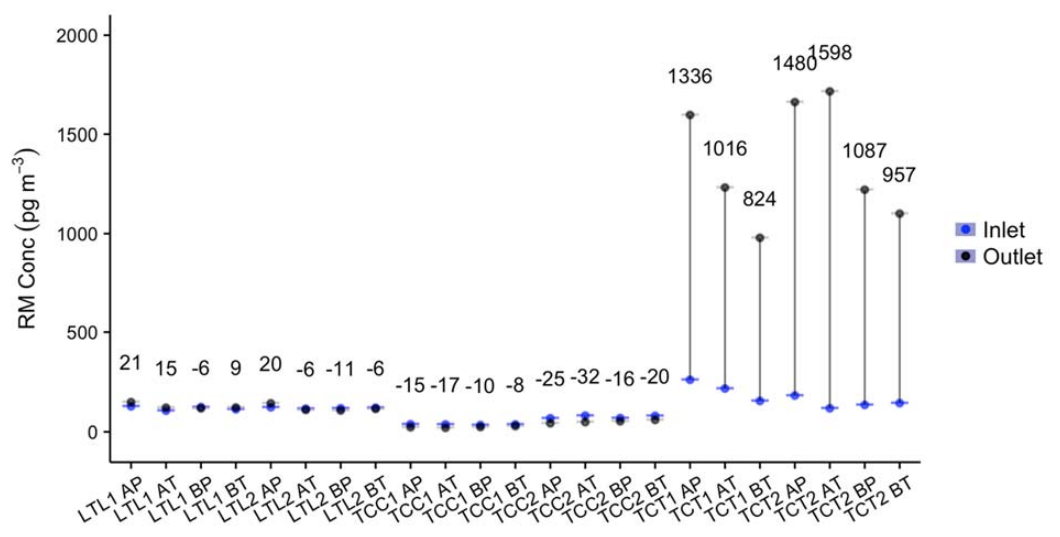


Figure 5. Expanded set of GOM flux measurements for select materials during summer. ΔC_{GOM} was below detection for 5 of 8 LTL measurements, and 2 of 8 TCC measurements, and these values were excluded.



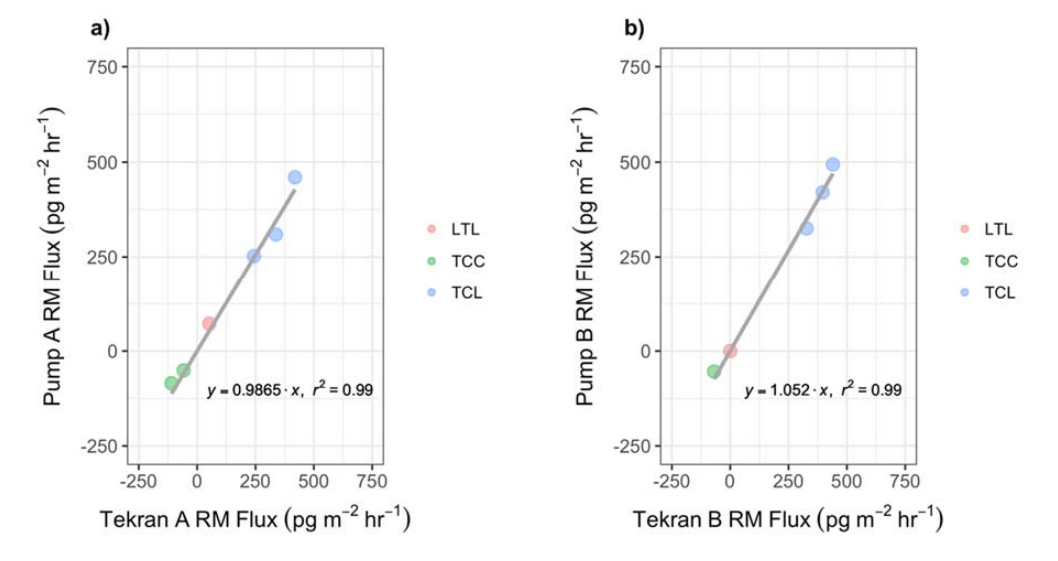


Figure 6. Comparison of GOM fluxes measured by Tekran controlled flow sample lines and external pump flow controlled sample lines, for a) System A and b) System B using TCL, TCC, LTL, and TCT summer measurements. Note TCT data not graphed, as fluxes were an order of magnitude higher and skew the regression r^2 towards 1.

Atmos. Meas. Tech. Discuss., https://doi.org/10.5194/amt-2018-360 Manuscript under review for journal Atmos. Meas. Tech. Discussion started: 30 November 2018 © Author(s) 2018. CC BY 4.0 License.





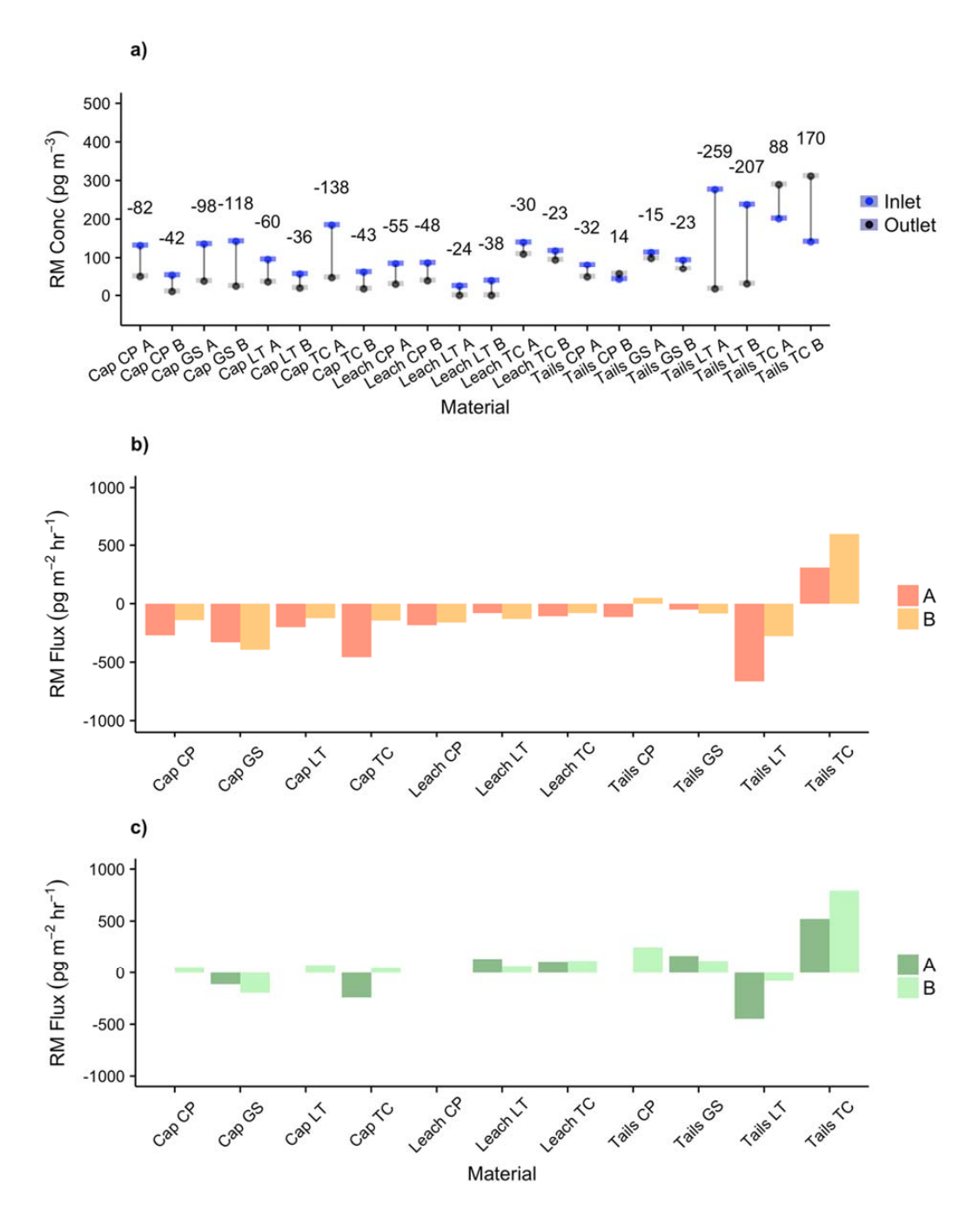


Figure 7. GOM flux measurements for all materials, winter 2016. a) ΔC_{GOM} , above detection limit for all measurements b) GOM flux, no chamber blank correction (shaded orange) c) GOM flux, with chamber blank correction (shaded green).

Manuscript under review for journal Atmos. Meas. Tech.

Discussion started: 30 November 2018 © Author(s) 2018. CC BY 4.0 License.





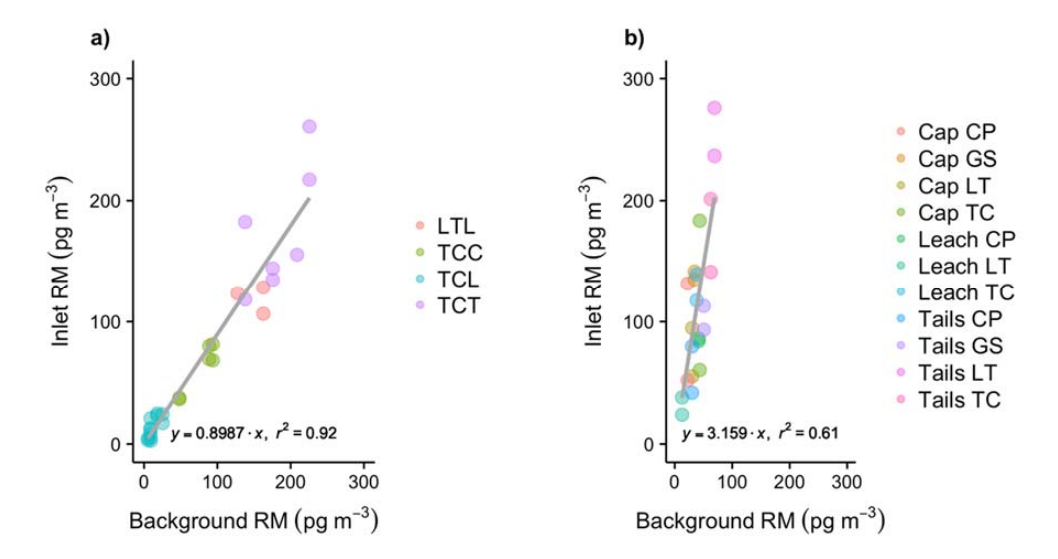


Figure 8. Comparison of ambient background GOM concentrations measured at 2 m height in the greenhouse, vs GOM concentrations measured at the chamber inlet, for a) Summer 2015, and b) Winter 2016. Background vs inlet concentrations were comparable during Summer measurements, but inlet concentrations were much higher relative to background in the winter.

Atmos. Meas. Tech. Discuss., https://doi.org/10.5194/amt-2018-360 Manuscript under review for journal Atmos. Meas. Tech. Discussion started: 30 November 2018 © Author(s) 2018. CC BY 4.0 License.





N	/laterial	Sample	Date	Substrate Conc (ng g 1)	GEM Flux (ng m² h¹)	RM Flux (ng m ² h ⁻¹)	RM Inlet (ng m ³)	RM V _d (cm s ⁻¹)	Ambient RM (ng m ³)	Temp (°C)	RH (%)	Solar (W m ⁻²)	Soil Temp
		TCL1*	5/16-5/19		134	0.29	0.01	-	0.01				
	Leach	TCL2*	5/19-5/22	11900	151 215	0.45	0.03	-	0.03 0.01	na	na	na	na
		TCL3*	5/22-5/25			0.37	0.02	-					
	Сар	TCC1A P		- 230	10	-0.05	0.04	0.04		22.6	41.6	15.8	23.9
		TCC1A T	7/21-7/23			-0.06	0.04	0.04	0.05				
		TCC1B P			12	na	0.03	na					
		TCC1B T				na	0.04	na					
		TCC2A P			4	-0.09	0.07	0.03	0.09	24.8	28.7	15.8	26.4
		TCC2A T TCC2B P	7/29-7/31			-0.11 -0.05	0.08 0.07	0.04 0.02					
		TCC2B T				-0.03	0.07	0.02					
		LTL1A P				0.07	0.08	0.02					
	Leach	LTLIA T			105	0.05	0.13	-	0.16	23.8	30.2	17.4	26.5
2		LTL1B P	8/12-8/14		87	na	0.11	na					
Summer 2013		LTLIB T				na	0.11	na					
		LTL2A P		- 590 -	100	0.07	0.12	-	0.13	23.4	24.1	17.3	25.6
, I		LTL2A T				na	0.12	na					
		LTL2B P	8/14-8/16		99	na	0.12	na					
		LTL2B T				na	0.12	na					
	Tailings	TCT1A P		- 35750 -	100	4.46	0.26	-	0.22	23.8	31.4	16.6	24.2
		TCT1A T	0/26 0/20		483	3.37	0.22	-					
		TCT1B P	8/26-8/28		370	na	0.15	-					
١,		TCT1B T				2.76	0.16	-					
Ι'		TCT2A P		- 33/30	702 457	5.02	0.18	-	0.16	22.0	33.3	13.9	22.1
		TCT2A T	8/28-8/31			5.43	0.12	-					
		TCT2B P	0/20=0/31			3.02	0.13	-					
		TCT2B T				2.57	0.14						
	Cap	TCCA	1/6/16	230	1	-0.24	0.18	0.07	0.04	15.0	37.6	2.7	14.5
		TCCB	170710	230	1	0.05	0.06	Ē					
		LTCA	1/7/16	150 120	0	0.00	0.09	-	0.03	14.5	38.6	9.7	11.8
		LTCB			-1	0.07	0.06	-					
		CPCA	1/20/16		-1	0.00	0.13	-					
		CPCB			na	0.06	0.05	-					
		GSCA	1/21/16	200	-1	-0.12	0.13	0.02	0.03	14.6	26.6	11.0	15.8
H		GSCB			-1 29	-0.20	0.14	0.04					
	Leach	TCLA TCLB	1/26/16	11900	30	0.11 0.11	0.14 0.12	-	0.04	13.4	35.3	9.3	15.2
3		CPLA		310	-18	0.11	0.12	-	0.04	13.9	34.9	16.5	15.3
Willies 2010		CPLB	1/29/16		-13	0.00	0.09	·=·					
2		LTLA			-4	0.13	0.02		0.01	11.7	25.5	14.6	14.2
		LTLB	2/2/16	590	-3	0.13	0.02	_					
\vdash	Tailings	CPTA		21150	4	0.00	0.08	-			37.5		
		CPTB	2/9/16		5	0.25	0.04	-	0.03	14.1		18.9	15.7
		GSTA		6960	16	0.16	0.11	-					13.8
		GSTB	2/10/16		-1	0.11	0.09	-	0.05 14.	14.4	39.3	11.6	
1		LTTA	2/27:::	11000	2	-0.45	0.28	0.05	0.07	19.8	23.1	31.0	22.3
		LTTB	3/20/16	11020	2	-0.08	0.24	0.01					
		TCTA	2/22/15		51	0.52	0.20	-	0.00	15.0		2- :	10.0
1		TCTB	3/22/16	35750	71	0.79	0.14	_	0.06	17.0	26.6	37.4	19.3

Table I. Summary of GEM and GOM flux and ambient parameters for all measurements. Fluxes are chamber blank-corrected where applicable, and V_d values are based on corrected fluxes (- indicates no deposition, na indicates non-detectable flux).